Journal of Sound and Vibration (2001) **248**(4), 763–767
doi:10.1006/jsvi.2001.3641, available online at http://www.idealibrary.com on IDEAL®

COMMENTS ON "REGULAR AND CHAOTIC DYNAMIC ANALYSIS AND CONTROL OF CHAOS OF AN ELLIPTICAL PENDULUM ON A VIBRATING BASEMENT"

R. VAN DOOREN

Department of Mechanical Engineering, Free University of Brussels, Pleinlaan 2, *B*-1050 *Brussels, Belgium. E-mail*: *rvdooren@vub.ac.be*

(*Received* 26 *January* 2001)

In reference [1], Ge and Lin studied the non-linear dynamics and control of an elliptical pendulum on a vibrating basement. The pendulum is assumed to be a particle with mass m_B connected to a block with mass m_A. The angular damping of the system is of the Van der Pol type. The vertical vibration of the horizontal plane is characterized by a periodic excitation having an amplitude A and frequency ω. Let x_A be the displacement of the block and ϕ the angle between the vertical axis and the pendulum. With the definitions $x_1 = x_A$, $x_2 = \dot{x}_A$, $x_3 = \phi$ and $x_4 = \dot{\phi}$, the equations of motion can be written as [1]

$$
\begin{aligned}
\dot{x}_1 &= x_2,\\
\dot{x}_2 &= [l x_4^2 \sin x_3 + (g/\Omega^2)\ \sin x_3 \cos x_3 - (k_2/\Omega m_B) x_2 + (k_1/\Omega m_B l)(x_3^2 - 1)\, x_4 \cos x_3\\
&\qquad - A(\omega/\Omega)^2 \sin x_3 \cos x_3 \sin(\omega\tau/\Omega)]/(a - \cos^2 x_3),\\
\dot{x}_3 &= x_4,\\
\dot{x}_4 &= [\,-(ag/\Omega^2 l)\sin x_3 - x_4^2 \sin x_3 \cos x_3 - (ak_1/\Omega m_B l^2)\ (x_3^2 - 1)\, x_4 + (k_2/\Omega m_B l) x_2\\
&\qquad \cos x_3 + (Aa\omega^2/\Omega^2 l)\sin x_3 \sin(\omega\tau/\Omega)]/(a - \cos^2 x_3),
\end{aligned}
\tag{1}
$$

where g is the gravitational acceleration, l is the distance between the block and the particle, and a and Ω are defined by

$$a = (m_A + m_B)/m_B, \qquad \Omega = (1/2\pi)\,[(m_A + m_B) g/m_A l]^{1/2}.$$

The following numerical values of the parameters have been chosen: $a = 3$, $g = 9{\cdot}8$, $\Omega = 0{\cdot}863$, $k_1 = 0{\cdot}25$, $k_2 = 0{\cdot}3$, $m_B = 1$, $\omega = 1$, $l = 0{\cdot}5$. The parameters k_1 and k_2 characterize the damping effects (angular and horizontal). Ge and Lin reported numerical results for the phase plots, period-T maps, bifurcation diagrams, power spectrum, Liapunov exponents and basins of attraction for the amplitude A of the periodic excitation varying between $A = 12{\cdot}4$ and $12{\cdot}6$, to investigate periodic and chaotic motion. They obtained $1T$-periodic motion for $A = 12{\cdot}4$, $2T$-periodic motion for $A = 12{\cdot}5$ with further period doublings and chaotic behavior for $A = 12{\cdot}6$. A very interesting part of their work was concerned with the control of chaotic motion.

0022-460X/01/490763 + 05 \$35.00/0 © 2001 Academic Press

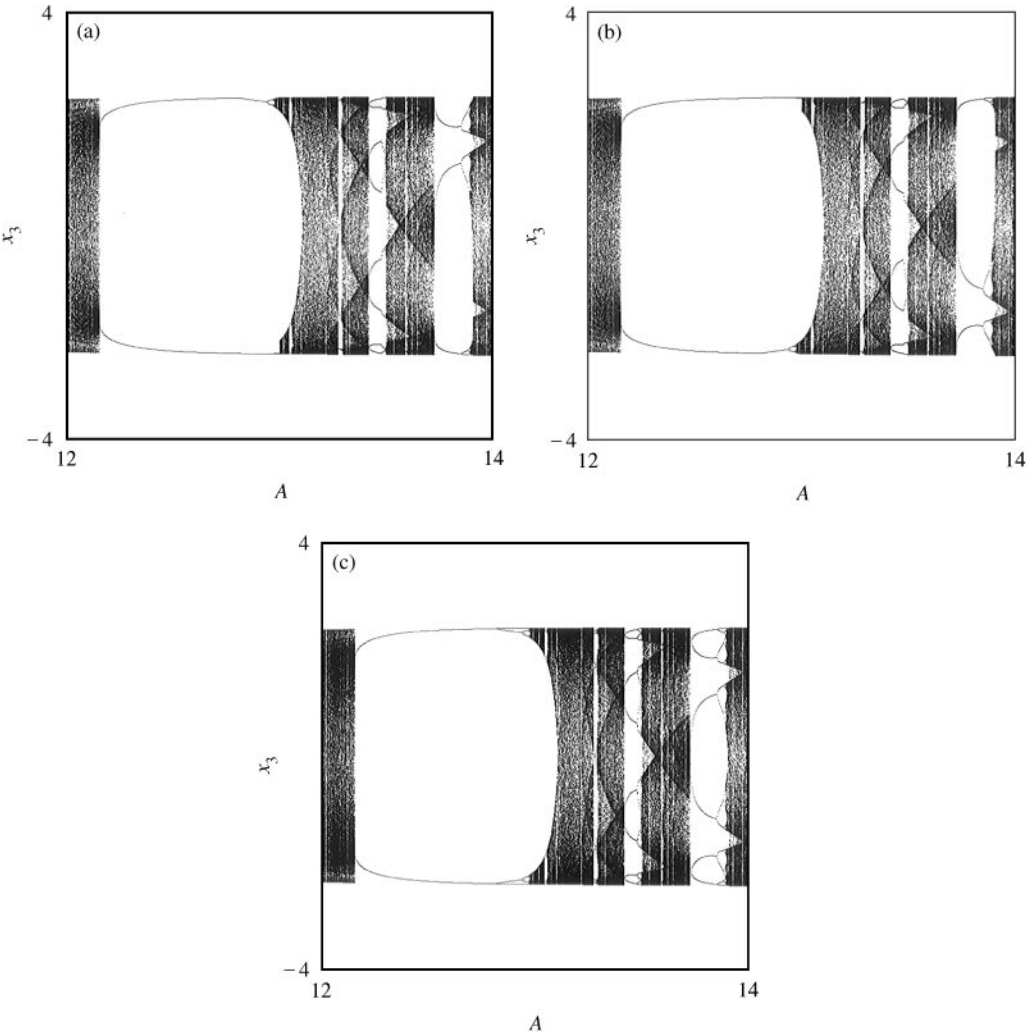

Figure 1. The bifurcation diagram for x_3 in the range $12 \leqslant A \leqslant 14$: (a) including motion of Type I; (b) including motion of Type II; (c) full diagram.

By investigating the system (1) with the numerical values of the parameters mentioned above, the author found some discrepancies with the results reported in reference [1]. Therefore, the bifurcation diagram for the angle $x_3 = \phi$ has been established for A varying from $A = 12$ to 14. Deleting the transient regime, the Poincaré section points for x_3 at multiples of the period $T = 2\pi\Omega/\omega$ of the excitation with respect to the parameter A are plotted. Taking a first set of initial values for x_1, x_2, x_3 and x_4, Figure 1(a) shows a very rich pattern of alternating periodic and chaotic motions. At $A \approx 12{\cdot}16$ a $2P$-periodic solution is created. Its Fourier series includes only odd harmonics (symmetric solution). At $A \approx 12{\cdot}82$ a slight indent appears in the upper branch. The solution becomes asymmetric retaining the same period. This $2P$-solution (called solution of Type I) bifurcates to a $4P$-solution at $A \approx 12{\cdot}94$. Further doublings occur with resulting chaotic behavior at $A \approx 12{\cdot}972$. With another choice for the initial conditions, the bifurcation diagram in Figure 1(b) is obtained.

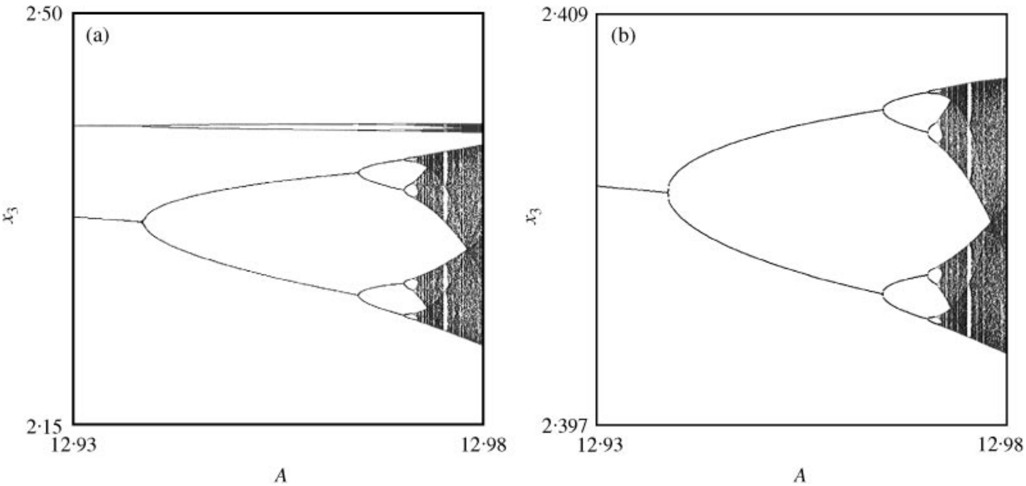

Figure 2. Cascade of period-doubling bifurcations in the range $12{\cdot}93 \leqslant A \leqslant 12{\cdot}98$: (a) for $2{\cdot}15 \leqslant x_3 \leqslant 2{\cdot}50$; (b) for $2{\cdot}397 \leqslant x_3 \leqslant 2{\cdot}409$.

Now at $A \approx 12{\cdot}82$ the indent appears on the lower branch continued by further period-doubling solutions and chaotic behavior at $A \approx 12{\cdot}972$ (solutions of Type II). The full bifurcation diagram consists of the superposition of both Figures 1(a) and (b) and is represented in Figure 1(c). The parts from Figures 1(a) and (b) for $12{\cdot}16 \leqslant A \leqslant 12{\cdot}82$ are coincident. At $A \approx 12{\cdot}82$ the single $2T$-solution is continued by two coexisting $2T$-solutions. Each of the latter solutions undergoes a period doubling at $A \approx 12{\cdot}94$. One of the splittings can only be seen by magnification.

Figure 2(a) yields a magnification of a small part of Figure 1(c) for A ranging from 12·93 to 12·98 with x_3 varying between 2·15 and 2·50 i.e., in the upper band. Two sequences of period-doubling bifurcations occur. Hereby the distances between two consecutive transition values diminish in accordance with Feigenbaum's relation [2]. Figure 2(b) is a magnification of the upper part of Figure 2(a) whereby x_3 varies between 2·397 and 2·409 with the same range for A.

The conclusions derived from the bifurcation diagram 1(c) differ from those derived from Figure 4 in reference [1]. The motion at $A = 12{\cdot}4$ is $2P$-periodic (mentioned as $1P$-periodic in reference [1]) and the bifurcation tree is found in the region from $A = 12{\cdot}93$ to 12·98 (mentioned from $A = 12{\cdot}4$ to 12·6 in Figure 4, reference [1]).

The results obtained by the author are confirmed by applying one of the most reliable criteria for determining the coexistence of periodic or chaotic attractors namely the study of their basins of attraction. As explained in reference [3] one chooses a grid of initial conditions in the phase and one integrates the system (1) for each set of initial conditions. Thus, one determines the periodic and chaotic attractors which are reached by the orbit. Different gray levels are assigned to each initial condition in conjunction with the relevant attractor that is approached. Figures 3(a) and (b) show the basins of attraction for the cases with $A = 12{\cdot}93$ and 12·98 respectively. They are obtained by using Nusse and Yorke's package DYNAMICS [4] with a 400×400 grid of pixels in the regions $-\pi \leqslant x_3 \leqslant \pi$ and $-4{\cdot}5 \leqslant x_4 \leqslant 4{\cdot}5$ (taking $x_1 = 1$ and $x_2 = 0$). In each case there are two coexisting basins. The domains of attraction are marked in light gray for motion of Type I and in dark gray for motion of Type II. For $A = 12{\cdot}93$ two periodic attractors occur both with the period $2T$. The Poincaré section points at $t = 0$ have symmetric positions in the x_3x_4-plane and are

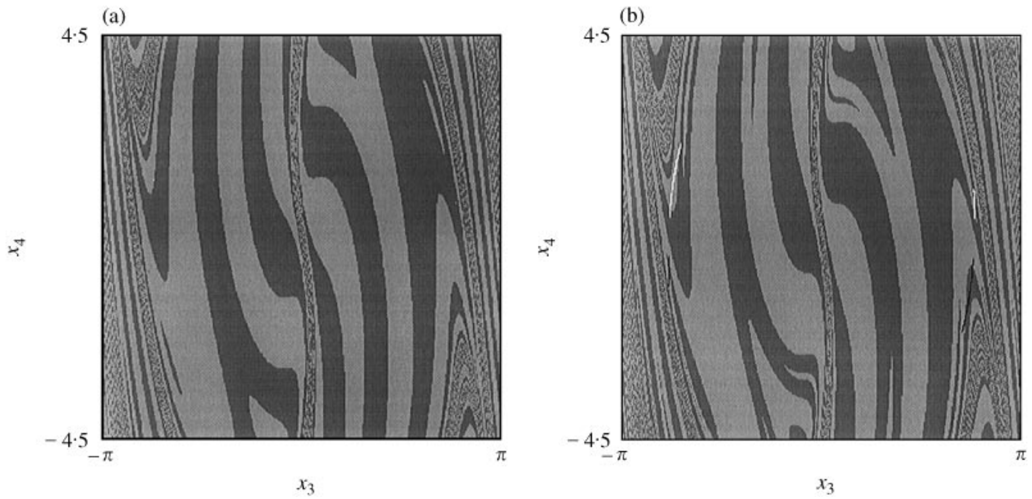

Figure 3. Basins of attraction in the phase plane x_3x_4 with $-\pi \leqslant x_3 \leqslant \pi$ and $-4{\cdot}5 \leqslant x_4 \leqslant 4{\cdot}5$: (a) $A = 12{\cdot}93$ (two coexisting periodic attractors both having the period $2T$); (b) $A = 12{\cdot}98$ (two coexisting chaotic attractors indicated in black and in white). Used gray levels for basins: light gray for motion of Type I and dark gray for motion of Type II.

given by

$$\text{Type I} \quad (2{\cdot}3265, -1{\cdot}2873), (-2{\cdot}4040, -0{\cdot}7834),$$

$$\text{Type II} \quad (2{\cdot}4040, 0{\cdot}7834), (-2{\cdot}3265, 1{\cdot}2873).$$

Fractal areas in the initial condition plane x_3x_4 occur near $x_3 = 0$ and near $x_3 = \pm\pi$. The pattern of the basins of attraction as represented in Figure 3(a) is rather similar for all cases with A varying from 12·82 to 12·98 in the sequences of the period-doubling bifurcations. For the case $A = 12{\cdot}98$ (see Figure 3(b)) two coexisting chaotic attractors, generated by consequent period-doubling bifurcations starting with $2T$-periodic motion, are found. Both chaotic attractors consist of two parts and are represented in black and in white.

For $A = 12{\cdot}4$ and 12·5 the author obtains a single basin of attraction filling the whole x_3x_4-plane under consideration whereby the two Poincaré section points represent one single $2T$-solution.

Hence, the results for the basins of attraction confirm our findings on the bifurcation diagrams reported above. In their comment on Figure 7(a) for $A = 12{\cdot}4$, Ge and Lin [1] mention the occurrence of two stable periodic solutions, both having the period $1T$. They used the modified interpolated cell mapping method [5].

The numerical results obtained by the use of the package DYNAMICS [4] have been confirmed by applying the numerical techniques explained in reference [6] based on the Runge–Kutta–Hŭta method [7] of order six which is a very accurate integration scheme.

REFERENCES

1. Z. M. Ge and T. N. Lin 2000 *Journal of Sound and Vibration* **230**, 1045–1068. Regular and chaotic dynamic analysis and control of chaos of an elliptical pendulum on a vibrating basement.
2. M. J. Feigenbaum 1980 *Los Alamos Science* **1**, 4–27. Universal behavior in nonlinear systems.

3. C. PEZESHKI and E. H. DOWELL 1988 *Physica D* **32**, 194–209. On chaos and fractal behavior in a generalized Duffing's system.
4. H. E. NUSSE and J. A. YORKE 1998 *Dynamics: Numerical Explorations*. New York: Springer; second edition.
5. Z. M. GE and S. C. LEE 1997 *Journal of Sound and Vibration* **199**, 189–206. A modified interpolated cell mapping.
6. R. VAN DOOREN 1996 *Chaos, Solitons and Fractals* **7**, 77–90. Chaos in a pendulum with forced horizontal support motion: a tutorial.
7. J. D. LAMBERT 1973 *Computational Methods in Ordinary Differential Equations*. Chichester: John Wiley.